

An infinite family of $bc8$ -like metastable phases in silicon

Vladimir E. Dmitrienko* and Viacheslav A. Chizhikov†
*A. V. Shubnikov Institute of Crystallography, FSRC “Crystallography
and Photonics” RAS, Leninskiy Prospekt 59, 119333, Moscow, Russia*

We show that new silicon crystalline phases, observed in the experiment with the laser-induced microexplosions in silicon crystals (Rapp *et al.* Nat. Commun. **6**, 7555 (2015)), are all superstructures of a disordered high-symmetry phase with $Ia\bar{3}d$ cubic space group, as well as known for many years phases $bc8$ (Si-III) and $r8$ (Si-XII). The physics of this phenomenon is rather nontrivial: The $bc8$ -like superstructures appear as regularly ordered patterns of switchable atomic strings, preserving everywhere the energetically favorable tetrahedral coordination of silicon atoms. The variety of superstructures arises because each string can be switched between two states independently of the others. An infinite family of different phases can be obtained this way and a number of them are considered here in detail. In addition to the known $bc8$, $bt8$, and $r8$ crystals, 128 tetrahedral structures with 16 (6 phases), 24 (22 phases), and 32 (100 phases) atoms per primitive cell are generated and studied, most of them are new ones. For the coarse-grain description of the structures with two possible states of switchable strings, the black/white (switched/nonswitched) Shubnikov symmetry groups has been used. An *ab initio* relaxation of the atomic positions and lattice parameters shows that all the considered phases are metastable and have higher density and energy relative to the $bc8$ phase at the ambient pressure. A possible scenario for appearance of those phases from the high-temperature amorphous phase is discussed.

PACS numbers:

I. INTRODUCTION

Despite the fact that our contemporary civilization is now based on one type of silicon crystals with the diamond structure, the diversity of crystal forms of this chemical element is not much inferior to that of carbon. There are numerous exotic structures with tetrahedral^{1,2} and more complicated atomic arrangements, including a big family of high-pressure silicon phases with higher coordinations³⁻⁵. The silicon phases are interesting first of all owing to their electronic properties and the latter are determined by details of the atomic structures and impurities. Another promising application is related to micro-electromechanical systems (MEMS)⁶ where the elastic properties of silicon are used. For all these purposes, one needs to look for new silicon-based crystals with the hope to find new unusual properties and applications.

One of the exotic tetrahedral structures, the $bc8$ phase, was discovered in 1963^{7,8}; its name means body-centered cubic with 8 atoms per primitive cell (that is 16 atoms per the body-centered cubic (bcc) unit cell, the lattice parameter $a = 6.64$ Å, and the space group is $Ia\bar{3}$). It is also called Si-III because it has been found after Si-I (diamond-like) and Si-II (β -Sn-like) silicon phases^{3,4}. All the atoms in $bc8$ are crystallographically equivalent, they are located at the three-fold axes, $16c$ positions (x, x, x) of group $Ia\bar{3}$ ($x \approx 0.1$), and have non-ideal tetrahedral coordination with one interatomic bond directed along

a three-fold cubic axis (A -bond) and three longer bonds (B -bonds) in non-symmetric directions. Structurally, the $bc8$ phase can be considered as the cubic arrangement of atomic strings directed along four $\langle 111 \rangle$ axes (this point is discussed in detail below). This phase was first obtained from the high-pressure β -Sn-like phase after pressure release^{7,8} and was found to be metastable at the ambient conditions. Its structural, thermodynamical, and electronic properties have been studied in detail for many years⁹⁻¹⁶. In the $bc8$ phase, like in diamond, there are only even-membered rings of interatomic bonds and the shortest rings are six-membered.

The first $bc8$ -like structure, $r8$ or Si-XII, was discovered in 1994¹⁷; $r8$ means rhombohedral with 8 atoms per unit cell, its space group is $R\bar{3}$, a subgroup of $Ia\bar{3}$. The structure of $r8$ appears from $bc8$ during a first-order pressure-induced structural transition as a result of breaking and rebonding of all the A -bonds directed along cubic direction $[111]$. Indeed, according to¹⁷, the rebonding can be understood as motion of the atom at (x, x, x) along direction $[111]$ of the $bc8$ unit cell until the A -bond to the atom at $(\bar{x}, \bar{x}, \bar{x})$ is broken and a new A -bond to the atom at $(\frac{1}{2} - x, \frac{1}{2} - x, \frac{1}{2} - x)$ is formed (Fig. 1). As a result of the rebonding, all the $[111]$ atomic strings are switched into another sequence of bonds preserving nevertheless the energetically favorable tetrahedral atomic arrangement. The phase transition is of the first order because the rebonding is accompanied by small but finite atomic displacements changing the topology of rings; in particular, five-membered rings appear in the $r8$ phase.

Both phases $bc8$ and $r8$ can also appear as a result of mechanical microindentation and their thermal relaxation back to the diamond silicon has been studied in numerous research works¹⁸⁻²¹. The electronic and optical properties of $bc8$ and $r8$ may have interesting practical

*email: dmitrien@crys.ras.ru

†email: chizhikov@crys.ras.ru

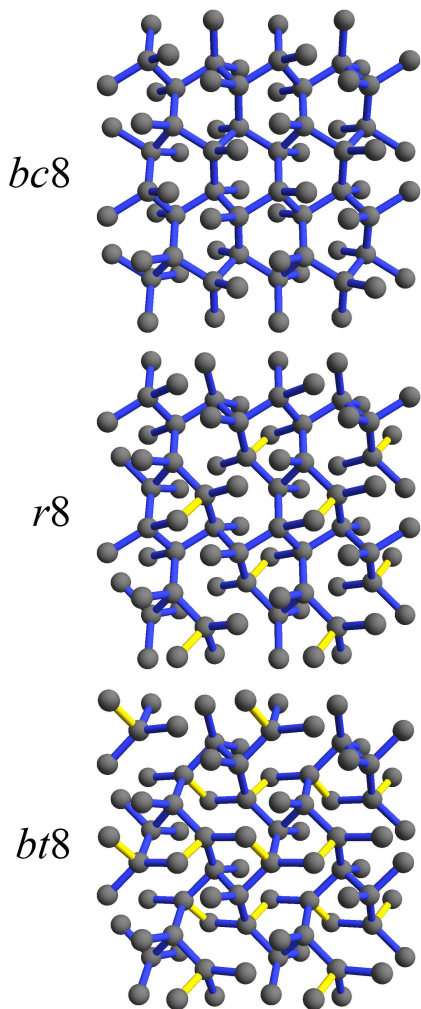


FIG. 1: (Color online) Comparison of the crystalline silicon structures $bc8$, $r8$, and $bt8$. An atomic layer is chosen to be parallel to plane (100) of $bc8$. In the phases $r8$ and $bt8$, the bonds coinciding with those of $bc8$ are shown in blue, and the new switched bonds along the $\langle 111 \rangle$ directions are yellow. The most dissimilar phases $bc8$ and $bt8$ differ by switching one eighth of the total number of bonds.

applications (see^{22,23} and references therein).

In 1999, it was shown^{24,25} that the rebonding mechanism found by Crain *et al.*¹⁷ is rather universal: in the $bc8$ structure, any set of the atomic strings can be independently switched without violation of tetrahedral coordination. In particular, a new tetragonal silicon phase ($bt8$) was predicted, where all the strings of $bc8$ parallel to two cubic diagonals (say $[111]$ and $[\bar{1}\bar{1}\bar{1}]$) were switched and those parallel to $[\bar{1}\bar{1}\bar{1}]$ and $[\bar{1}\bar{1}\bar{1}]$ were not (Fig. 1). The space symmetry of $bt8$ is $I4_1/a$ and it is not a subgroup of $Ia\bar{3}$: there are new symmetry elements, fourfold screw axes, relating switched and non-switched strings. The $bt8$ structure demonstrates the maximum density of five-membered bond rings²⁵ and its electronic properties are expected to be rather different from those of $bc8$, $r8$, and

diamond phases. Energetics and structural relaxation of $bt8$ have been studied *ab initio* both for silicon²⁵ and carbon²⁶. It has been shown that at the ambient pressure $bt8$ is more dense than $bc8$ and $r8$ and it becomes energetically more favorable than $bc8$ and $r8$ at pressures above 13 GPa where the β -tin silicon structure is, in fact, more favorable than all the $bc8$ -like phases. Later on, in 2013, the $bt8$ phase was independently reinvented and studied *ab initio* for silicon and germanium²⁷ and for carbon as well²⁸ (in the latter case the symmetry was claimed to be $I4_1$ whereas the calculated atomic coordinates corresponded in fact to the more symmetric $I4_1/a$ space group). The $bc8$ -like structures were also studied by algebraic geometry²⁹ and by the high-dimensional projection methods used for quasicrystals and their approximants³⁰.

The real breakthrough happened in 2015 when Rapp *et al.*³¹ found evidence for several metastable silicon phases after ultrashort laser-induced confined microexplosions³² at the interface between a transparent amorphous silicon dioxide layer (SiO_2) and an opaque single-crystal Si substrate. They determined the lattice parameters and possible atomic structures of the following phases: $bt8$, $st12$ (analog of $st12$ in germanium), two tetragonal phases with 32 atoms per unit cells, and some others. For description of the structures they used an *ab initio* random structure search³³. It should be noted that one of the 32-atoms tetragonal phases was found independently³⁴ using the ideas of metadynamics and evolutionary algorithms. The exotic silicon phases like $bc8$, $r8$, and those new discovered by Rapp *et al.*³¹ have provided a novel insight into the local structure and properties of the amorphous phase of silicon^{9,10,24,35}.

In the present paper we suggest a unified description of all new silicon crystalline phases (except $st12$) observed by Rapp *et al.*³¹ and numerous similar phases. Those complicated phases are shown to be the $bc8$ -like structures with periodically switched strings, like in the simple case of $r8$. As a result, the lattice vectors of those phases are some periods of $bc8$. In addition to known $bc8$, $r8$, and $bt8$, we generate a complete set of $bc8$ -like phases with 16, 24, and 32 atoms per primitive cells and relax their structures *ab initio*.

II. BC8 STRUCTURE AND STRING SWITCHING

As mentioned in the introduction, the atomic structure of the $bc8$ phase can be considered as a set of atomic strings parallel to the threefold axes of the cubic space group $Ia\bar{3}$, no. 206. Here the string structure is described in detail (Fig. 2). All atoms are located in the position of $16c$ (x, x, x), $x = x_w \approx 0.1$, with threefold point symmetry, and each string possesses two nonequivalent inversion centers in the positions of $8a$ ($0, 0, 0$) and $8b$ ($\frac{1}{4}, \frac{1}{4}, \frac{1}{4}$). In $bc8$ all strings are equivalent to each other. Let us consider one of them, say, that parallel to axis $[111]$ and passing through the origin $(0, 0, 0)$. Then its atoms have

coordinates $(\frac{n}{2}, \frac{n}{2}, \frac{n}{2}) \pm (x_w, x_w, x_w)$, where n is an arbitrary integer. The A -bonds between neighboring atoms of the string are $(2x_w, 2x_w, 2x_w)$ and they alternate with next-neighbor distances A' ($\frac{1}{2} - 2x_w, \frac{1}{2} - 2x_w, \frac{1}{2} - 2x_w$). Therefore the string of atoms looks like a sequence of alternating A -bonds centered at inversion centers $(\frac{n}{2}, \frac{n}{2}, \frac{n}{2})$, and approximately 1.5 times longer stretches A' centered at inversion centers $(\frac{1}{4} + \frac{n}{2}, \frac{1}{4} + \frac{n}{2}, \frac{1}{4} + \frac{n}{2})$, (Fig. 2b). The string of this type will be called *white*, hence the subindex w .

However, there is another value of x , $x = x_b = \frac{1}{4} - x_w$, which gives an identical $bc8$ structure rotated relative to the former by $\frac{\pi}{2}$ around a twofold axis (the subindex b means *black*). The black and white $bc8$ structures can be also transformed one to another by small local shifts of atoms along threefold directions resulting in breaking/switching of A -bonds, as suggested by Crain *et al.*¹⁷ for the $r8$ phase and described above in the introduction. In the string picture, the rebonding means simply that A' and A -bonds are locally permuted (switched), Fig. 2c. Thus, for the black $bc8$, in the considered above string [111] the A -bonds are centered at $(\frac{1}{4} + \frac{n}{2}, \frac{1}{4} + \frac{n}{2}, \frac{1}{4} + \frac{n}{2})$, whereas A' at $(\frac{n}{2}, \frac{n}{2}, \frac{n}{2})$.

An important observation is that any set of strings can be independently switched between black and white states without violation of energetically favorable tetrahedral coordination^{24,25}. The tetrahedral coordination means that each atom has four neighbors, the lengths of bonds are not very different, and all interbond angles exceed $\frac{\pi}{2}$. An example of bond length and angle statistics can be found below in Section V. The switching of a single isolated string in the perfect $bc8$ structure has been simulated *ab initio*²⁵ and it has been found that it costs less than 0.02 eV per atom.

Since every string is allowed to be switched independently of the others, there exist 2^N different combinations of switching, where the total number of strings N is proportional to the surface area of a crystal. This huge number of possible structures arises from the purely combinatorial consideration, without taking into account their physical properties. Note that all members of the infinite family of $bc8$ -like crystals have a similar topological structure. Indeed, the string switching affects only the bonds lying along the four axes of type $\langle 111 \rangle$. Any $bc8$ -like phase can be obtained from $bc8$ by switching at most one half of A -bonds, i.e. one eighth of the total number of bonds (Fig. 1).

As mentioned above, the rotation of $bc8$ by $\frac{\pi}{2}$ changes the color of all atomic strings. This means that different combinations of switching can define the same structure. For example, the two cases when all atomic strings have the same color, (w, w, w, w) or (b, b, b, b) , correspond to a single structure, namely $bc8$. Further, if the strings parallel to any two threefold axes are white, and those parallel to remaining two axes are black (the cases (w, w, b, b) , (w, b, w, b) , *etc.*), then the crystal symmetry becomes tetragonal, and identical $bt8$ phases with different orientations of the tetragonal axis are obtained. Finally, if

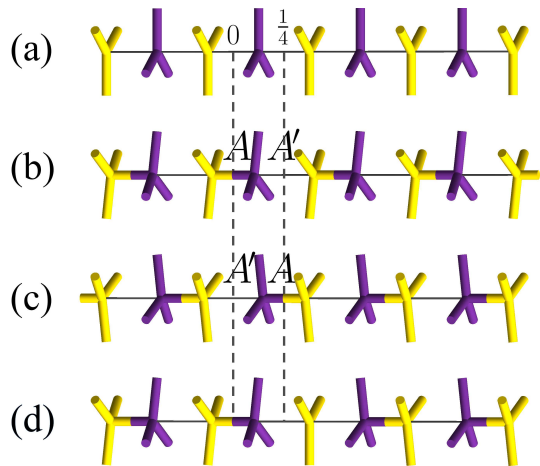


FIG. 2: (Color online) An atomic string in the structure of $bc8$ -like silicon. Each atom has one A -bond along the string and three B -bonds with atoms of other strings. The string can be switched from the mean position (a), corresponding to the structure with space group $Ia\bar{3}d$, to one of two extreme states, white (b) and black (c). Switching from white to black permutes the A -bonds with A' -distances, preserving tetrahedral atomic arrangement. In addition, the string can be split into white and black parts, separated by defects (d). The switching process may consist in moving such a defect along the string³⁶.

the sign of the strings parallel to any threefold axis is opposite to the sign of other strings (the cases (w, w, w, b) , (w, b, b, b) , *etc.*) then identical $r8$ phases arise with different orientations of the rhombohedral axis. The three phases, $bc8$, $bt8$, and $r8$, exhaust the list of $bc8$ -like structures with the minimal primitive cell containing 8 atoms. Their common feature is that parallel strings have the same color.

In spite of the obvious connection of the phases $bc8$ and $bt8$, there is no group-subgroup relation between them. We can assume the existence of a supersymmetric phase with space group $Ia\bar{3}d$, which is a supergroup for both $Ia\bar{3}$ and $I4_1/a$. An evident way to construct the superphase is to turn all the strings into the half-switched state. In this case, all atoms are located in the position of $16b$ of group $Ia\bar{3}d$ with three-coordinated graphene-like environment (Fig. 2a). However, this environment is not favorable for the silicon atoms. Another, more physical way to obtain a supersymmetric phase is to switch every string randomly to one of two possible states, white or black (Figs. 2b, 2c). In this case, the $Ia\bar{3}d$ symmetry is a result of disorder²⁴, and the phase transition to $bc8$, $r8$, $bt8$, or a more complicated structure is of disorder-order type.

III. BC8-LIKE SUPERSTRUCTURES WITH ENLARGED PRIMITIVE CELLS

A more complicated *bc8*-like phase with larger primitive cell can occur if the structure contains parallel atomic strings of different colors. The primitive cell of the phase is a multiple in volume and number of atoms to the *primitive* cell of *bc8*, and its Bravais lattice is a subset of the *bcc* Bravais lattice of *bc8*. In addition, each Bravais lattice corresponds to several different phases due to multiple ways to color the strings passing through its primitive cell. In order to enumerate and classify the structures with the same Bravais lattice, we need to calculate the number of independent, i.e. not connected by periodicity, strings in each of the four directions $\langle 111 \rangle$. This number is proportional to the volume of the primitive cell and inversely proportional to the smallest lattice period along the direction. For example, the number N_{111} of independent strings parallel to axis $[111]$ is equal to the greatest common divisor of three triple products

$$\begin{aligned} n_a &= (1, 1, 1) \cdot [\mathbf{b} \times \mathbf{c}], \\ n_b &= (1, 1, 1) \cdot [\mathbf{c} \times \mathbf{a}], \\ n_c &= (1, 1, 1) \cdot [\mathbf{a} \times \mathbf{b}], \end{aligned} \quad (1)$$

where \mathbf{a} , \mathbf{b} , and \mathbf{c} are the Bravais lattice periods, expressed in the parameters of the initial *bcc* lattice.

The numbers $N_{\bar{1}\bar{1}\bar{1}}$, $N_{\bar{1}\bar{1}\bar{1}}$, and $N_{\bar{1}\bar{1}\bar{1}}$ can be calculated in the same way. Further, the combinatorial number of possible two-colorings of strings is equal to $2^{N_{111}+N_{\bar{1}\bar{1}\bar{1}}+N_{\bar{1}\bar{1}\bar{1}}+N_{\bar{1}\bar{1}\bar{1}}}$, however, the actual number of different phases is significantly less. For example, in the case of the smallest primitive cell ($N_{111} = N_{\bar{1}\bar{1}\bar{1}} = N_{\bar{1}\bar{1}\bar{1}} = N_{\bar{1}\bar{1}\bar{1}} = 1$), sixteen possible combinations of switching define only three different phases, *bc8*, *bt8*, and *r8*. This significant reduction in the number of different structures is due to two reasons. First, some structures can be connected by the elements of group $Ia\bar{3}d$ not included in the own space group of the structures. Second, some combinations of switching can define structures with smaller primitive cells.

Table I shows the currently known *bc8*-like phases of silicon. Recently, several new structures were experimentally observed, with primitive cells two and four times larger than that of *bc8*³¹. They are listed in the bottom part of the table, with the names being written according to Ref.³¹ as well as in our own notation (in parentheses). Along with conventional space groups of the crystals, we also indicate the black and white (Shubnikov) groups, the meaning of which will be explained later in Section IV. The last column shows the unit cell periods expressed in the parameters of the initial *bcc* lattice. The phases listed in Table I, unlike some others (diamond, *st12*, etc.), belong to the same family and can be described in the language of string switching, Figs. 3–5.

The list from Table I is far from being exhaustive. As a first goal, we would like to find all the similar structures with double, triple, and quadruple cells, containing 16, 24, and 32 silicon atoms, respectively. First we find

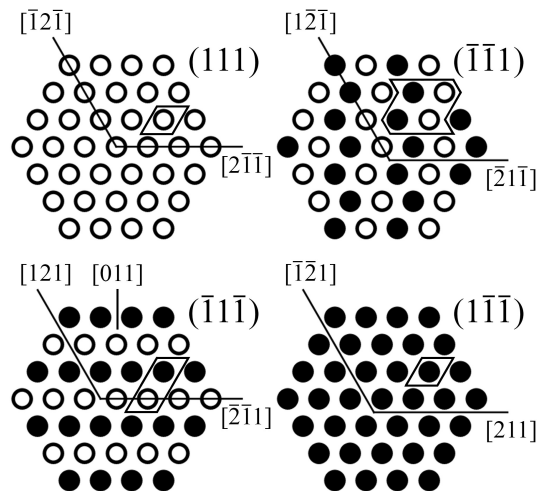


FIG. 3: Atomic strings in phase *m32* (*m32-8*) in projections onto the planes $\{111\}$ perpendicular to them. For each projection its 2D generating cell is shown. White and black circles indicate the switching of strings. For projections $(\bar{1}\bar{1}\bar{1})$ and $(\bar{1}\bar{1}\bar{1})$ the string switching alternates along the perpendicular directions $[011]$ and $[\bar{2}\bar{1}\bar{1}]$, correspondingly.

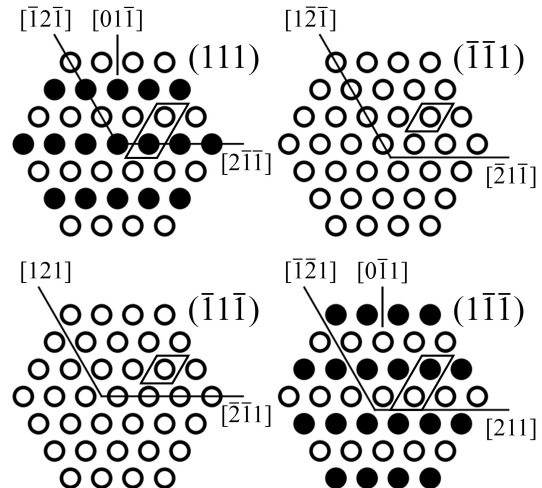


FIG. 4: Atomic strings in phase *m32** (*sm16-2*). For projections (111) and $(\bar{1}\bar{1}\bar{1})$ the string switching alternates along the same direction $[01\bar{1}]$.

all the Bravais lattices with the specified cell volumes, which are subsets of the initial *bcc* lattice. Then, all possible structures are obtained by the enumeration of two-colorings of the independent strings.

In order to avoid double counting, we discard the structures with smaller primitive cells. For example, all the structures with basis vectors (100) , (010) , and (001) (lattice 16-2 in Table II) actually have a two times smaller primitive cell, and therefore they coincide with the phases *bc8*, *bt8*, and *r8*. Thus, it turns out that some lattices

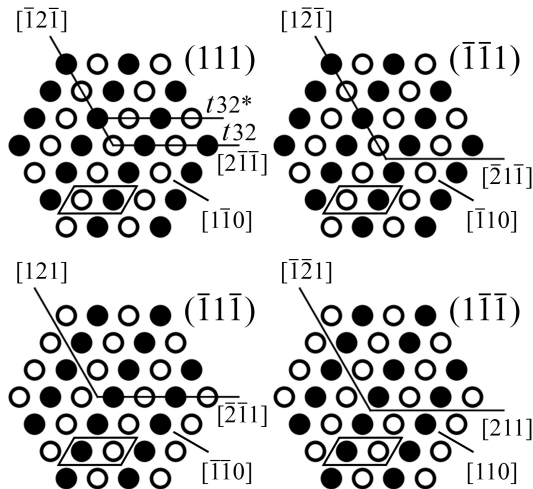


FIG. 5: Atomic strings in phases $t32$ ($t32-1$) and $t32^*$ ($t32-3$). Both phases are characterized by alternation of the string switching along the perpendicular directions $[110]$ and $[\bar{1}\bar{1}0]$. Phase $t32^*$ differs from $t32$ by the inverse switching of all the strings parallel to axis $[111]$.

generate no new phases. It is also possible that different combinations of switching define the structures connected to each other by symmetry transformations. Such identical structures are also discarded. The statistical results of the search are summarized in Table II. Seven lattices (one with double, two with triple, and four with quadruple primitive cells) give rise to 128 structures (or 177 if we consider chiral enantiomorphs as different phases), four of which are listed in Table I. The supplemental material contains the list of all the new phases and crystallographic information files (CIFs) with atomic coordinates³⁷.

IV. THE MAGNETIC ANALOGY

Let us define the operation of *conjugation* as the simultaneous switching of all strings. As mentioned above, for the phases $bc8$, $bt8$, and $r8$ the conjugation is equivalent to a rotation of the crystal as a whole and it does not lead to appearance of a new phase. The question arises whether this is a common property of the $bc8$ -like structures? The answer is no, and already among the crystals with a double primitive cell we find two different triclinic structures, $a16-3$ and $a16-4$, conjugated to each another. Note that this operation does not affect the elements of spatial symmetry and therefore both phases are of the same space group. Nevertheless, their physical properties (energy, atomic density, cell parameters, etc.), generally speaking, should differ.

In order to prove that conjugated structures have the same space group, an analogy with magnetic crystals can be suggested. Let us assign to each atom the shift vector

from a symmetric graphene-like position of group $Ia\bar{3}d$ to its real position with tetrahedral coordination. This vector is always parallel to the threefold axis (string) passing through the atom, whereas its direction alternates along the string. The situation resembles the ordering of magnetic moments arranged in the nodes of the original $Ia\bar{3}d$ phase, provided that they are involved in two strong magnetic interactions: (i) a spin-orbit interaction, forcing the moments to align along the easy magnetization axes coinciding with strings; (ii) an antiferromagnetic exchange between neighboring atoms on the strings. It is obvious that in this analogy the conjugation plays the role of the time reversal operation, which in turn is independent of spatial symmetry. Therefore, it does not change the space group of the structure.

Note that the analogy is not complete, because, in contrast to a magnetic moment, the atomic position shift changes sign upon inversion and remains the same upon time reversal. As for the strings, it is easy to see that they change their color upon rotations of 90° and keep it unchanged for all other rotations of point group $m\bar{3}m$, as well as for inversion. For example, the xyz -component of a magnetic octupole moment behaves in a similar way. Using the magnetic analogy we can extend the space group of a $bc8$ -like phase by adding symmetry elements conjugating its structure. Then, the symmetry of the phase will be described by a Shubnikov magnetic group^{38–40}. Thus, the magnetic groups of the phases $bc8$, $bt8$, and $r8$ are $Ia\bar{3}d'$, $I4_1/ac'd'$, and $R\bar{3}c'$, correspondingly (Table I). In the supplemental material all $bc8$ -like crystals are classified both by space and magnetic groups³⁷.

V. MICROSCOPIC STRUCTURE AND PHYSICAL PROPERTIES

Let us now consider some structural features of the $bc8$ -like phases and their correlation with physical properties such as energy and atomic density. As mentioned above, each atom has one A -bond along the string passing through it, and three B -bonds with atoms on other strings. Therefore, two kinds of angles between the bonds can be distinguished, the α angle between bonds A and B , and the β angle between two B -bonds. In the real structures, all the bonds tend to be of the same size. It is achieved when the A - and B -bonds have lengths of about $\sqrt{2}/4 \approx 0.35$ lattice parameters of $bc8$, and the A' -distances are about $(2\sqrt{3} - \sqrt{2})/4 \approx 0.51$ parameters of $bc8$. In such ideal structure, the values of α and β are determined by the colors of the neighboring strings. Thus, depending on switching, the angles α are subdivided into $\alpha' \approx 98.5^\circ$ and $\alpha'' \approx 94.3^\circ$, and the angles β into $\beta_1 \approx 107.0^\circ$, $\beta_2 \approx 117.9^\circ$, $\beta'_2 \approx 119.5^\circ$, and $\beta_3 \approx 130.6^\circ$ (Fig. 6). The statistical variation of the angles calculated from the structural data from Ref.³¹ is shown using Gaussian distributions. It is seen that the angles α , β_1 , β_2 , and β_3 are well distinguished. Appar-

ently, the angles α , which are close to 90° , have an excess energy, and the structure should undergo an additional distortion in order to increase them.

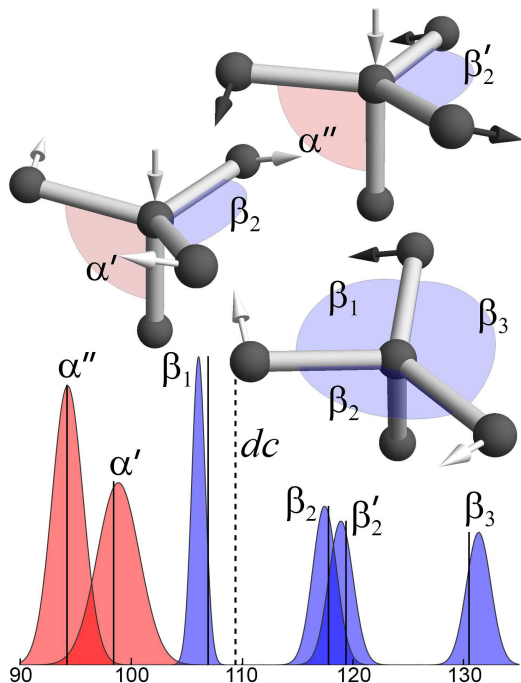


FIG. 6: (Color online) The angles between interatomic bonds in the $bc8$ -like structures depending on switching of adjacent strings. The directions of switching are shown by the white/black arrows. The angles α are between bonds A and B , and the angles β are between B -bonds. In the plot, the Gaussians approximate statistical data on the real $bc8$ -like crystals from Ref.³¹. The vertical lines correspond to the ideal structure with the length of A -bonds equal to $\sqrt{2}/4 \approx 0.35$ lattice parameters of $bc8$. The dashed line indicates the angle between bonds in diamond structure, $\arccos(-1/3) \approx 109.5^\circ$.

An important characteristic of tetrahedral structures is the statistics of atomic rings. All the considered $bc8$ -like phases have a girth (i.e. the length of a shortest ring) equal to five, except for $bc8$ itself, which is made up exclusively of six-membered rings. For the first approximation, we can investigate the dependence of physical properties on the amount of five-membered rings per atom, which varies from $\nu_5 = 0$ for $bc8$ to $\nu_5 = 1$ for $bt8$. Fig. 7 shows dependencies of the energy and volume per atom on the value of ν_5 for several $bc8$ -like phases, calculated during *ab initio* simulations of the structural relaxation of the phases, performed with QUANTUM ESPRESSO package^{41,42} (see details of the DFT modeling in the supplemental material³⁷). It is seen that when the frequency of five-membered rings grows, both the energy and atomic density increase. The positive correlation between ν_5 and energy per atom seems to be explained by the relation between five-membered rings and the “bad” angles α'' . Indeed, from geometrical considerations we can express the frequencies of different

interbond angles through ν_5 : $\nu_{\alpha'} = 3 - 2\nu_5$, $\nu_{\alpha''} = 2\nu_5$, $\nu_{\beta_1} = \nu_{\beta_2'} = \nu_{\beta_3} = \nu_5$, $\nu_{\beta_2} = 3 - 3\nu_5$.

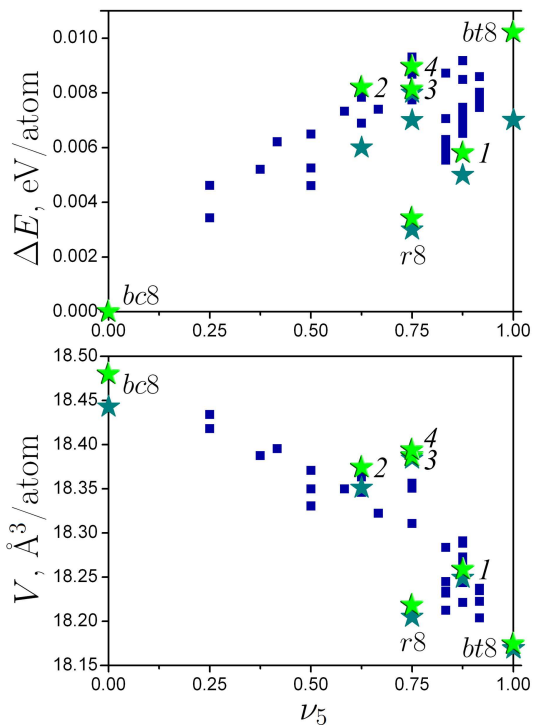


FIG. 7: (Color online) The energy and volume per atom for $bc8$ -like structures depending on the frequency of five-membered rings calculated *ab initio*; the stars indicate experimentally observed structures, green for our results and dark cyan for the data from Ref.³¹: 1 — $m32$ ($m32-8$), 2 — $m32^*$ ($sm16-2$), 3 — $t32$ ($t32-1$), 4 — $t32^*$ ($t32-3$); the squares correspond to some new structures described in the present paper³⁷. The energy is measured from that of $bc8$.

All $bc8$ -like phases are close to each other but differ from other silicon phases. For example, the belonging of a given structure to the family can easily be determined by comparing its periods to those of the bcc lattice, and by the number of atoms in the unit cell multiple of eight. Furthermore, all these phases have similar energy and atomic density. It was recently found that the Raman spectra of some unidentified silicon phases obtained in the experiment with the laser-induced microexplosions resemble the spectra of the phases $bc8$, $r8$, and $bt8$, although the correspondence is not exact⁴³. Here, the existence of an infinite series of intermediate phases may be one of the possible explanations for the discrepancy.

VI. DISCUSSION AND CONCLUSIONS

In summary, we described in detail the physical mechanism behind the complicated silicon structures observed by Rapp *et al.* after ultrashort laser microexplosions³¹. Those silicon phases (except $st12$) can be obtained from

the phase $bc8$ by switching the $\langle 111 \rangle$ atomic strings in different regular (periodic) ways. The stochastic switching of the strings gives a disordered phase with $Ia\bar{3}d$ cubic symmetry, and the space groups of the $bc8$ -like phases are subgroups of $Ia\bar{3}d$. All the possible phase transitions between different $bc8$ -like phases should be of the first order (not continuous) because atoms of the switched strings jump over finite distances.

We have found possible rich polymorphism of $bc8$ -like phases, and to distinguish between them it would be very important to study carefully any small differences in diffraction patterns and in other physical properties (e.g. in the Raman spectra). In addition, the considered family of $bc8$ -like phases provides a good opportunity for studying the ability of existing empirical potentials to capture the structure and energetics of these phases and other complicated silicon materials (thanks to the Referee who attracted our attention to this option).

It would also be very interesting to use the technique of Rapp *et al.*³¹ for the $bc8$ crystals instead of diamond silicon because in this case new $bc8$ -like phases will grow on the parent $bc8$ matrix. Reasonably large (several mm size) phase-pure $bc8$ polycrystals have been grown recently by different methods^{44,45}.

Finally, we can propose a possible explanation for the observed polymorphism of $bc8$ -like phases based on the

ideas described above. It was shown in Ref.²⁵, that the reduced intensity functions (the structure-dependent parts of the X-ray scattering pattern), are very similar for amorphous silicon and for disordered polycrystalline $Ia\bar{3}d$ phase. Thus, we can suppose that the high-temperature/high-pressure amorphous phase first transforms into disordered $Ia\bar{3}d$ phase and then, depending on local temperature, pressure, and shear, into different $bc8$ -like phases for which $Ia\bar{3}d$ is the parent phase. Therefore, quite probably, the $bc8$ -like phases should also appear after the laser-induced microexplosions on the interface between SiO_2 and amorphous silicon.

Acknowledgements

We are grateful to S. A. Pikin, S. M. Stishov, V. V. Brazhkin, M. V. Gorkunov, M. Kléman, V. S. Kraposhin, A. L. Talis, and C. J. Pickard for useful discussions and communications. This work was supported by the Ministry of Science and Higher Education of the Russian Federation within the State assignment FSRC “Crystallography and Photonics” RAS in part of symmetry analysis, and by the grant of Prezidium of Russian Academy of Sciences in part of computer simulations.

-
- ¹ J. Crain, G. J. Ackland, and S. J. Clark, Exotic structures of tetrahedral semiconductors. *Rep. Prog. Phys.* **58**, 705-54 (1995).
 - ² Q. Fan, C. Chai, Q. Wei, H. Yan, Y. Zhao, Y. Yang, X. Yu, Y. Liu, M. Xing, J. Zhang, and R. Yao, Novel silicon allotropes: Stability, mechanical, and electronic properties. *J. Appl. Phys.* **118**, 185704 (2015).
 - ³ G. J. Ackland, High-pressure phases of group IV and III-V semiconductors. *Rep. Prog. Phys.* **64**, 483-516 (2001).
 - ⁴ A. Mujica, A. Rubio, A. Muñoz, and R. J. Needs, High-pressure phases of group-IV, III-V, and II-VI compounds. *Rev. Mod. Phys.* **75**, 863-912 (2003).
 - ⁵ B. Haberl, T. A. Strobel, and J. E. Bradby, Pathways to exotic metastable silicon allotropes. *Appl. Phys. Rev.* **3**, 040808 (2016).
 - ⁶ M. Tilli, T. Motooka, V.-M. Airaksinen, S. Franssila, M. Paulasto-Kröckel, and V. Lindroos (eds.), *Handbook of Silicon Based MEMS Materials and Technologies - 2nd Edition* (Elsevier, 2015).
 - ⁷ R. H. Wentorf, Jr. and J. S. Kasper, Two new forms of silicon. *Science* **139**, 338-9 (1963).
 - ⁸ J. S. Kasper and S. M. Richards, The crystal structures of new forms of silicon and germanium. *Acta Cryst.* **17** 752-5 (1964).
 - ⁹ J. D. Joannopoulos and M. L. Cohen, Electronic properties of complex crystalline and amorphous phases of Ge and Si. I. Density of states and band structures. *Phys. Rev. B* **7**, 2644-57 (1973).
 - ¹⁰ J. D. Joannopoulos and M. L. Cohen, Electronic properties of complex crystalline and amorphous phases of Ge and Si. II. Band structure and optical properties. *Phys. Rev. B* **8**, 2733-55 (1973).
 - ¹¹ M. T. Yin, Si-III (BC-8) crystal phase of Si and C: Structural properties, phase stabilities, and phase transitions. *Phys. Rev. B* **30**, 1773-6 (1984).
 - ¹² R. Biswas, R. M. Martin, R. J. Needs, and O. H. Nielsen, Stability and electronic properties of complex structures of silicon and carbon under pressure: Density-functional calculations. *Phys. Rev. B* **35**, 9559-68 (1987).
 - ¹³ V. V. Brazhkin, A. G. Lyapin, S. V. Popova, and R. N. Voloshin, Solid-phase disordering of bulk Ge and Si samples under pressure. *JETP Lett.* **56**, 152-156 (1992).
 - ¹⁴ J. Crain, S. J. Clark, G. J. Ackland, M. C. Payne, V. Milman, P. D. Hatton, and B. J. Reid, Theoretical study of high-density phases of covalent semiconductors. I. *Ab initio* treatment. *Phys. Rev. B* **49**, 5329-40 (1994).
 - ¹⁵ S. J. Clark, G. J. Ackland, and J. Crain, Theoretical study of high-density phases of covalent semiconductors. II. Empirical treatment. *Phys. Rev. B* **49**, 5341-52 (1994).
 - ¹⁶ H. Zhang, H. Liu, K. Wei, O. O. Kurakevych, Y. Le Godec, Z. Liu, J. Martin, M. Guerrette, G. S. Nolas, and T. A. Strobel, BC8 silicon (Si-III) is a narrow-gap semiconductor. *Phys. Rev. Lett.* **118**, 146601 (2017).
 - ¹⁷ J. Crain, G. J. Ackland, J. R. Maclean, R. O. Piltz, P. D. Hatton, and G. S. Pawley, Reversible pressure-induced structural transitions between metastable phases of silicon. *Phys. Rev. B* **50**, 13043-46 (1994).
 - ¹⁸ S. V. Demishev, D. G. Lunts, D. V. Nekhaev, N. E. Sluchanko, N. A. Samarin, V. V. Brazhkin, A. G. Lyapin, S. V. Popova, and N. N. Mel'nik, Structural relaxation of the metastable Kasper phase of silicon. *JETP* **82**, 1159 (1996).

- ¹⁹ V. Domnich and Y. Gogotsi, Phase transformations in silicon under contact loading. *Rev. Adv. Mater. Sci.* **3**, 1-36 (2002).
- ²⁰ B. Haberl, M. Guthrie, S. V. Sinogeikin, G. Shen, J. S. Williams, and J. E. Bradby. Thermal evolution of the metastable r8 and bc8 polymorphs of silicon. *High Pressure Research.* **35**, 99-116 (2015).
- ²¹ S. Wong, B. C. Johnson, B. Haberl, A. Mujica, J. C. McCallum, J. S. Williams, and J. E. Bradby, Thermal evolution of the indentation-induced phases of silicon. *J. Appl. Phys.* **126**, 105901 (2019).
- ²² B. D. Malone, J. D. Sau, and M. L. Cohen, Ab initio study of the optical properties of Si-XII, *Phys. Rev. B* **78**, 161202 (2008).
- ²³ S. Wong, B. Haberl, B. C. Johnson, A. Mujica, M. Guthrie, J. C. McCallum, J. S. Williams, and J. E. Bradby, Formation of an r8-dominant Si material, *Phys. Rev. Lett.* **122**, 105701 (2019).
- ²⁴ V. E. Dmitrienko and M. Kléman, Icosahedral order and disorder in semiconductors. *Phil. Mag. Lett.* **79**, 359-67 (1999).
- ²⁵ V. E. Dmitrienko, M. Kléman, and F. Mauri, Quasicrystal-related phases in tetrahedral semiconductors: Structure, disorder, and ab initio calculations. *Phys. Rev. B* **60**, 9383-9 (1999).
- ²⁶ V. E. Dmitrienko, M. Kleman, and F. Mauri, Silicon and carbon structures with icosahedral order, phason jumps, and disorder. *Ferroelectrics* **250**, 213-218 (2001).
- ²⁷ J.-T. Wang, C. F. Chen, H. Mizuseki, and Y. Kawazoe, Kinetic origin of divergent decompression pathways in silicon and germanium. *Phys. Rev. Lett.* **110**, 165503 (2013).
- ²⁸ T. Ishikawa, N. Suzuki, and K. Shimizu, Crystal structure searching by free energy surface trekking: application to carbon at 1 TPa. *J. Phys.: Conf. Ser.* **500**, 162003 (2014).
- ²⁹ V. S. Kraposhin, A. L. Talis, V. G. Kosushkin, A. A. Ogneva, and L. I. Zinober, Structures of the cubic and rhombohedral high-pressure modifications of silicon as packing of the rod-like substructures determined by the algebraic geometry. *Acta Cryst. B* **64**, 26-33 (2008).
- ³⁰ V. E. Dmitrienko and M. Kléman, Icosahedral order and disorder in tetrahedral semiconductors. Three-dimensional and six-dimensional views. *Mater. Sci. Eng.* **294-296**, 246-9 (2000).
- ³¹ L. Rapp, B. Haberl, C. J. Pickard, J. E. Bradby, E. G. Gamaly, J. S. Williams, and A. V. Rode, Experimental evidence of new tetragonal polymorphs of silicon formed through ultrafast laser-induced confined microexplosion. *Nat. Commun.* **6**, 7555 (2015).
- ³² L. Rapp, B. Haberl, J. E. Bradby, E. G. Gamaly, J. S. Williams, and A. V. Rode, Confined micro-explosion induced by ultrashort laser pulse at SiO₂/Si interface. *Appl. Phys. A* **114**, 33-43 (2014).
- ³³ A. Mujica, C. J. Pickard, and R. J. Needs, Low-energy tetrahedral polymorphs of carbon, silicon, and germanium. *Phys. Rev. B* **91**, 214104 (2015).
- ³⁴ Q. Zhu, A. R. Oganov, A. O. Lyakhov, and X. Yu, Generalized evolutionary metadynamics for sampling the energy landscapes and its applications. *Phys. Rev. B* **92**, 024106 (2015).
- ³⁵ S. Ruffell, J. Vedi, J. E. Bradby, and J. S. Williams, Effect of hydrogen on nanoindentation-induced phase transformations in amorphous silicon, *J. Appl. Phys.* **106**, 123511 (2009).
- ³⁶ See Supplemental Material at [URL] for the animated im-
- age of the string switching process.
- ³⁷ See Supplemental Material at [URL] for the description of new bc8-like phases with enlarged primitive cells and corresponding crystallographic information files (CIF).
- ³⁸ D. B. Litvin, *Magnetic group tables: 1-, 2-, and 3-dimensional magnetic subperiodic groups and magnetic space groups* (International Union of Crystallography, 2013).
- ³⁹ Bilbao Crystallographic Server, <http://www.cryst.ehu.es/>
- ⁴⁰ J. M. Perez-Mato, S. V. Gallego, E. S. Tasci, L. Elcoro, G. de la Flor, and M. I. Aroyo, Symmetry-based computational tools for magnetic crystallography. *Annu. Rev. Mater. Res.* **45**, 217 (2015).
- ⁴¹ QUANTUM ESPRESSO, <http://www.quantum-espresso.org/>
- ⁴² P. Giannozzi, S. Baroni, N. Bonini, M. Calandra, R. Car, C. Cavazzoni, D. Ceresoli, G. L. Chiarotti, M. Cococcioni, I. Dabo, A. Dal Corso, S. de Gironcoli, S. Fabris, G. Fratesi, R. Gebauer, U. Gerstmann, C. Gougousis, A. Kokalj, M. Lazzeri, L. Martin-Samos, N. Marzari, F. Mauri, R. Mazzarello, S. Paolini, A. Pasquarello, L. Paulatto, C. Sbraccia, S. Scandolo, G. Schlausero, A. P. Seitsonen, A. Smogunov, P. Umari, and R. M. Wentzcovitch, QUANTUM ESPRESSO: a modular and open-source software project for quantum simulations of materials. *J. Phys.: Condens. Matter* **21**, 395502 (2009).
- ⁴³ L. A. Smillie, M. Niihori, L. Rapp, B. Haberl, J. S. Williams, J. E. Bradby, C. J. Pickard, and A. V. Rode, Micro-Raman spectroscopy of ultrashort laser induced microexplosion sites in silicon. [arXiv:2003.14039](https://arxiv.org/abs/2003.14039) (2020).
- ⁴⁴ O. O. Kurakevych, Y. Le Godec, W. A. Crichton, J. Guignard, T. A. Strobel, H. Zhang, H. Liu, C. Coelho Diogo, A. Polian, N. Menguy, S. J. Juhl, and C. Gervais, Synthesis of bulk BC8 silicon allotrope by direct transformation and reduced-pressure chemical pathways. *Inorg. Chem.*, **55**, 8943-8950 (2016).
- ⁴⁵ X. Li, Z. Li, K. Yang, and D. He, Phase-pure bulk BC8 silicon prepared through secondary phase transition method under high pressure, *Materials Lett.* (2019).

TABLE I: The known $bc8$ -like phases of silicon

phase	Fedorov group	Shubnikov group	unit cell ideal periods
$bc8$	$Ia3$ (206)	$Ia3d'$ (230.148)	} (100), (010), (001)
$bt8$	$I4_1/a$ (88)	$I4_1/ac'd'$ (142.567)	
$r8$	$R\bar{3}$ (148)	$R\bar{3}c'$ (167.107)	$(\frac{1}{2}\frac{1}{2}\frac{1}{2})$, $(\frac{1}{2}\frac{1}{2}\frac{1}{2})$, $(\frac{1}{2}\frac{1}{2}\frac{1}{2})$
$m32$ ($m32$ -8)	$P2_1/c$ (14)	$P2_1/c$ (14.75)	$(\frac{1}{2}\frac{1}{2}\frac{1}{2})$, (011), $(\frac{3}{2}\frac{1}{2}\frac{1}{2})$
$m32^*$ ($sm16$ -2)	$C2$ (5)	$C22'2'$ (21.41)	(100), (011), (011)
$t32$ ($t32$ -1)	$P\bar{4}2_1c$ (114)	$P_C\bar{4}2_1c$ (114.281)	} (110), (110), (001)
$t32^*$ ($t32$ -3)	$P4_32_12$ (96)	$P_C4_32_12$ (96.149)	

TABLE II: The supercells multiple to the primitive cell of $bc8$ and the number of possible $bc8$ -like structures

cell name	basis vectors (periods of bcc lattice)	multiplicity	number of structures without/with enantiomorphs	the known structures
8-1	$(\frac{1}{2}, \frac{1}{2}, \frac{1}{2})$, $(\frac{1}{2}, \frac{1}{2}, \frac{1}{2})$, $(\frac{1}{2}, \frac{1}{2}, \frac{1}{2})$	1	3/3	$bc8$, $r8$, $bt8$
16-1	$(\frac{1}{2}, \frac{1}{2}, \frac{1}{2})$, $(\frac{1}{2}, \frac{1}{2}, \frac{1}{2})$, $(1, 0, \bar{1})$	2	6/8	$m32^*$
16-2	$(1, 0, 0)$, $(0, 1, 0)$, $(0, 0, 1)$	2	—	
24-1	$(\frac{1}{2}, \frac{1}{2}, \frac{1}{2})$, $(\frac{1}{2}, \frac{1}{2}, \frac{1}{2})$, $(\frac{3}{2}, \frac{1}{2}, \frac{3}{2})$	3	18/23	$t32$, $t32^*$
24-2	$(\frac{1}{2}, \frac{1}{2}, \frac{1}{2})$, $(0, \bar{1}, 1)$, $(1, 0, \bar{1})$	3	4/4	
24-3	$(1, 0, 0)$, $(0, 1, 0)$, $(\frac{1}{2}, \frac{1}{2}, \frac{3}{2})$	3	—	
32-1	$(1, 0, 0)$, $(0, 1, 1)$, $(0, 1, 1)$	4	6/8	
32-2	$(\frac{1}{2}, \frac{1}{2}, \frac{1}{2})$, $(\frac{1}{2}, \frac{1}{2}, \frac{1}{2})$, $(2, 0, \bar{2})$	4	46/68	$m32$
32-3	$(\frac{1}{2}, \frac{1}{2}, \frac{1}{2})$, $(1, 0, \bar{1})$, $(\frac{1}{2}, \frac{3}{2}, \frac{1}{2})$	4	22/26	
32-4	$(\frac{3}{2}, \frac{1}{2}, \frac{1}{2})$, $(\frac{1}{2}, \frac{3}{2}, \frac{1}{2})$, $(\frac{1}{2}, \frac{1}{2}, \frac{3}{2})$	4	26/40	
32-5	$(1, 0, 0)$, $(0, 1, 0)$, $(0, 0, 2)$	4	—	
32-6	$(1, 0, 1)$, $(0, 1, 1)$, $(0, \bar{1}, 1)$	4	—	
32-7	$(1, 0, 1)$, $(1, 1, 0)$, $(0, 1, 1)$	4	—	
32-8	$(1, 0, \bar{1})$, $(0, 1, 0)$, $(\frac{1}{2}, \frac{1}{2}, \frac{3}{2})$	4	—	
			Total: 131/180	

SUPPLEMENTAL MATERIAL

Animated GIFs

Animation *bondon.gif* demonstrates a probable mechanism of the string switching from white to black and back. The process involves moving a dangling interatomic bond along a 3-fold axis, which can be associated with a quasi-particle called “bondon”. Note that the sign of switching does not correlate with the direction of bondon movement.

Crystallographic information files

For generation and enumeration of possible *bc8*-like phases we use an approach based on the “ideal” atomic structure of the *bc8* phase as a crystalline approximant of icosahedral quasicrystals where the switches of the string correspond to phasonic jumps of atoms^{24,26,30}. In this case, the *A* and *B* interatomic bonds are parallel, correspondingly, to three- and fivefold axes of an icosahedron, with the ratio of bonds $r_B/r_A = \sqrt{(\tau + 2)}/3 \approx 1.098$ ($\tau = (1 + \sqrt{5})/2$ is the golden mean). When the string is switched, the *A* bonds remains of the same length and the third type of bonds (*C*-bonds) appears, connecting atoms at switched and non-switched strings.

The folder *cifs.zip* contains Crystallographic Information Files (CIFs) with atomic coordinates in such ideal representation. The cell parameters are calculated based on the ideal *bc8* crystal period $a = 6.658\text{\AA}$. Note that the crystal lattices of the idealized structures are characterized by the unit cell parameters (angles, ratio of periods) characteristic of the cubic lattice of the *bc8* phase. A real structure may have slightly distorted cell parameters if phase symmetry allows it. The files from the folder *cifs.zip* describe the structures as having the least symmetrical group *P1*. All positions are listed for the primitive cell. Some of the structures have been relaxed using *ab initio* simulations. In these cases, the cif-file, tagged by an extra underscore symbol, also contains the refined crystallographic data. The *cifs.zip* file can be sent by request.

Details of ab initio simulation

For the *ab initio* DFT relaxation of the initial “ideal” *bc8*-like structures we used the QUANTUM ESPRESSO code^{41,42}. We selected the generalized gradient approximation (GGA) with the Perdew–Burke–Ernzerhof (PBE) exchange-correlation functional which seems to provide better agreement between experimental and theoretical lattice parameters than the local density approximation (LDA). We used the ultra-soft pseudopotential *Si.pbe-nrkkjus-psl.1.0.0.UPF*⁴¹, the plane-wave energy cutoff of 40 Ry, and the structural relaxations were supposed to

be converged when all of the interatomic forces were less than 10^{-3} Ry/a.u. The *bc8*-like structures relaxed this way are presented in the cif-files tagged by an extra underscore symbol in the file names. This includes all *bc8*-like structures with the lattices 16-1, 24-1, 24-2, 32-1, the monoclinic phases *m32*-6,7,8 with the lattice 32-3, and the rhombohedral phases *r32*-3,4,5,6 with the lattice 32-4.

Lattices and structures

Below 131 *bc8*-like phases are listed and classified (180 with chiral enantiomorphs). The list exhausts all similar structures with 8, 16, 24, and 32 atoms in primitive cells, including previously known ones (*bc8*, *bt8*, *r8*, *m32*-8 (*m32*³¹), *sm16*-2 (*m32*^{*31}), *t32*-1 (*t32*³¹), *t32*-3 (*t32*^{*31})), and 124 structures proposed for the first time.

The description of structures corresponds to the following scheme.

Lattice type. The phases described are divided into eight different lattices: one each with 8 and 16 atoms in primitive cell, two with 24 atoms, and four with 32 atoms. Every lattice is defined by periods, which coincides with some periods of the *bcc* lattice of the *bc8* crystal. The type of Bravais lattice is indicated.

Symmetry. The structures of *bc8*-like phases are classified by their symmetry. Crystals with the same symmetry are combined together. Listed are the space groups, the Pearson symbols, and the black-white magnetic groups (in red) of the structures.

Structures. The name of each phase is constructed according to the *csN-n* scheme, where the optional symbol *c* means centering (*b*: body-centered, *s*: base-centered), *s* indicates crystal system (*a*: triclinic, *m*: monoclinic, *t*: tetragonal, *r*: rhombohedral, *h*: hexagonal, *c*: cubic), *N* is the number of atoms in the primitive cell, *n* is the sequence number. For a chiral structure, its enantiomorph is indicated in parentheses.

LATTICE 8

PERIODS: $a(\frac{1}{2}, \frac{1}{2}, \frac{1}{2})$, $a(\frac{1}{2}, \frac{1}{2}, \frac{1}{2})$, $a(\frac{1}{2}, \frac{1}{2}, \frac{1}{2})$

BRAVAIS LATTICE: body-centered cubic

STRUCTURES:

$Ia\bar{3}$ (206); *cI16*; $Ia\bar{3}d'$ (230.148) : *bc8*

$I4_1/a$ (88); *tI16*; $I4_1/ac'd'$ (142.567) : *bt8*

$R\bar{3}$ (148); *hR24*; $R\bar{3}c'$ (167.107) : *r8*

LATTICE 16-1

PERIODS: $a(\frac{1}{2}, \frac{1}{2}, \frac{1}{2})$, $a(\frac{1}{2}, \frac{1}{2}, \frac{1}{2})$, $a(1, 0, \bar{1})$

BRAVAIS LATTICE: base-centered orthorhombic

STRUCTURES:

$C2$ (5); $mC32$; $C2'2'2'$ (21.41) : $sm16-1(2)$
 $P2_1$ (4); $mP16$; $C2'2'2_1$ (20.33) : $m16-1(2)$
 $P\bar{1}$ (2); $aP16$;
 $P2'/c'$ (13.69) : $a16-1, a16-2$
 $P\bar{1}$ (2.4) : $a16-3, a16-4$

LATTICE 24-1

PERIODS: $a(\frac{1}{2}, \frac{1}{2}, \frac{1}{2})$, $a(\frac{1}{2}, \frac{1}{2}, \frac{1}{2})$, $a(\frac{3}{2}, \frac{1}{2}, \frac{3}{2})$
BRAVAIS LATTICE: face-centered orthorhombic

STRUCTURES:

$C2/c$ (15); $mC48$; $Fd'd'd$ (70.530) : $sm24-1, sm24-2$
 $C2$ (5); $mC48$; $F2'2'2$ (22.47) : $sm24-3(5), sm24-4(6)$
 $P\bar{1}$ (2); $aP24$;
 $C2'/c'$ (15.89) : $a24-1, a24-2, a24-3, a24-4, a24-5$
 $C2'/c'$ (15.89) : $a24-6, a24-7$
 $P\bar{1}$ (2.4) : $a24-8, a24-9, a24-10, a24-11$
 $P1$ (1); $aP24$; $C2'$ (5.15) : $a24-12(13), a24-14(15), a24-16(17)$

LATTICE 24-2

PERIODS: $a(\frac{1}{2}, \frac{1}{2}, \frac{1}{2})$, $a(0, \bar{1}, 1)$, $a(1, 0, \bar{1})$
BRAVAIS LATTICE: hexagonal

STRUCTURES:

$P\bar{3}$ (147); $hP24$; $P\bar{3}c'1$ (165.95) : $h24-1, h24-2$
 $P\bar{1}$ (2); $aP24$: $C2'/c'$ (15.89) : $a24-18, a24-19$

LATTICE 32-1

PERIODS: $a(1, 0, 0)$, $a(0, 1, 1)$, $a(0, \bar{1}, 1)$

BRAVAIS LATTICE: tetragonal

STRUCTURES:

$P\bar{4}2_1c$ (114); $tP32$; $P_C\bar{4}2_1c$ (114.281) : $t32-1$
 $P4_12_12$ (92); $tP32$; $P_C4_12_12$ (92.117) : $t32-2(3)$
 $P4_32_12$ (96); $tP32$; $P_C4_32_12$ (96.149) : $t32-3(2)$
 $C2/c$ (15); $mC64$; $C2/c$ (15.85) : $sm32-1, sm32-2$
 $P\bar{1}$ (2); $aP32$; $C2'/c'$ (15.89) : $a32-1$
 $P1$ (1); $aP32$; $P2'$ (3.3) : $a32-2(3)$

LATTICE 32-2

PERIODS: $a(\frac{1}{2}, \frac{1}{2}, \frac{1}{2})$, $a(\frac{1}{2}, \frac{1}{2}, \frac{1}{2})$, $a(2, 0, \bar{2})$

BRAVAIS LATTICE: base-centered orthorhombic

STRUCTURES:

$C2$ (5); $mC64$; $C2'2'2'$ (21.41) : $sm32-3(9), sm32-4(10), sm32-5(11), sm32-6(12), sm32-7(13), sm32-8(14)$
 $P2_1$ (4); $mP32$; $C2'2'2_1$ (20.33) : $m32-1(3), m32-2(4)$
 $P\bar{1}$ (2); $aP32$;
 $P2'/c'$ (13.69) : $a32-4, a32-5, a32-6, a32-7, a32-8, a32-9, a32-10, a32-11, a32-12, a32-13, a32-14, a32-15$
 $P\bar{1}$ (2.4) : $a32-16, a32-17, a32-18, a32-19, a32-20, a32-21, a32-22, a32-23, a32-24, a32-25, a32-26, a32-27$
 $P1$ (1); $aP32$;
 $C2'$ (5.15) : $a32-28(30), a32-29(31), a32-32(34), a32-33(35)$
 $P2'$ (3.3) : $a32-36(42), a32-37(43), a32-38(44), a32-39(45), a32-40(46), a32-41(47)$
 $P1$ (1.1) : $a32-48(52), a32-49(53), a32-50(54), a32-51(55)$

LATTICE 32-3

PERIODS: $a(\frac{1}{2}, \frac{1}{2}, \frac{1}{2})$, $a(1, 0, \bar{1})$, $a(\frac{1}{2}, \frac{3}{2}, \frac{1}{2})$

BRAVAIS LATTICE: monoclinic

STRUCTURES:

$P2_1/c$ (14); $mP32$; $P2_1/c$ (14.75) : $m32-5, m32-6, m32-7, m32-8$
 $P\bar{1}$ (2); $aP32$;
 $P2'/c'$ (13.69) : $a32-56, a32-57, a32-58, a32-59$
 $P2'_1/c'$ (14.79) : $a32-60, a32-61$
 $P\bar{1}$ (2.4) : $a32-62, a32-63, a32-64, a32-65, a32-66, a32-67, a32-68, a32-69$
 $P1$ (1); $aP32$;
 $P2'$ (3.3) : $a32-70(72), a32-71(73)$
 $P1$ (1.1) : $a32-74(76), a32-75(77)$

LATTICE 32-4

PERIODS: $a(\frac{3}{2}, \frac{1}{2}, \frac{1}{2})$, $a(\frac{1}{2}, \frac{3}{2}, \frac{1}{2})$, $a(\frac{1}{2}, \frac{1}{2}, \frac{3}{2})$

BRAVAIS LATTICE: rhombohedral

STRUCTURES:

$R\bar{3}$ (148); $hR96$; $R\bar{3}c'$ (167.107) : $r32-1, r32-2$
 $R3$ (146); $hR96$; $R32'$ (155.47) : $r32-3(5), r32-4(6)$
 $P\bar{1}$ (2); $aP32$;
 $C2'/c'$ (15.89) : $a32-78, a32-79, a32-80, a32-81, a32-82, a32-83$
 $P\bar{1}$ (2.4) : $a32-84, a32-85, a32-86, a32-87$

$P1$ (1); $aP32$

$C' (9.39)$: $a32-88(90)$, $a32-89(91)$

$C2' (5.15)$: $a32-92(98)$, $a32-93(99)$, $a32-94(100)$, $a32-$

$95(101)$, $a32-96(102)$, $a32-97(103)$

$P1 (1.1)$: $a32-104(108)$, $a32-105(109)$, $a32-106(110)$,
 $a32-107(111)$